Improving the image below complex overburden geology with FWI and Q-tomography: A case study at Etame license area, offshore Gabon

Richard Huang, Chong Chung, Benjamin Cole, Ivan Berranger, Ika Novianti, ION*
Paul Ware, Vaalco Energy

Summary

This paper discusses a velocity model building and imaging case study on a multi-azimuth towed streamer survey over the Etame license area in offshore Gabon. The model building and imaging strategy features refraction and reflection full waveform inversion (FWI), Q-tomography and Q-migrations (Q-RTM and Q-Kirchhoff PSDM). In combination with 3D deghosted input seismic data, we present the generation of accurate, high resolution and geologically consistent velocity models. In the presence of geophysical and geologic challenges, we show the workflow and techniques significantly improve the overall seismic image and the pre-salt targets which revives the oil development field.

Introduction

The Congo Basin, developed from the rifting and subsequent drifting of the African and South American continents, has drawn industry operators' attention for over half a century. In 1998, Vaalco and partners discovered Etame, located in the northern portion of the Congo Basin offshore southern Gabon, licensed it, and started developing production of the area. Its two main targets, Barremian and Early Aptian Dentale and Gamba sandstone formations, are both pre-salt. Gill and Cameron (2002) describe a number of challenges for seismic imaging over the area, including:

- "Salt walls" that are typically 1-2 km high, subparallel to the strike of the underlying rift faulting, and extend 10-50 km
- Complex overburden sequences, especially the Madiela carbonates with interval velocities that can vary rapidly from 4,000 m/s to 7,000 m/s over a short distance of a few kilometers

Due to the geologic challenges, past mapping of the Gamba sandstone underneath the salt wall has been unreliable. Over the last two decades, to improve the imaging of the target section and as the result of field development, several new acquisitions and processing/reprocessing were performed over the area. Nonetheless, a few critical difficulties are still present, limiting the appraisal of the prospect for further development, including:

- The legacy velocity model covering the acreage has multiple seams from various separate processing and imaging efforts, lacks well calibration, and does not fit well the geological model
- The resulting seismic image suffers from the velocity issues and exhibits a poor S/N ratio in various areas, most critically below salt

In 2020, Vaalco Gabon S.A acquired a towed streamer survey over the area, consisting of two azimuths. The water column depth is 75 m on average. The full-fold imaging area is about 750 km^2. Together with six legacy acquisitions contributing as a third azimuth, the objective was to obtain a high-fidelity seismic image to confirm the well locations of the upcoming drilling campaign and to enhance the potential of the pre-salt acreage. This will be accomplished through high resolution and geologically conformable velocity models, modern broadband multi-azimuth seismic processing and Q-imaging.

Method

The first challenge we faced is the data choice and conditioning for FWI. The shooting density (37.5 m flip-flap-flop shot spacing) and long offset (8 km) of the 2020 acquisition make it the preferred data for velocity model building. However, its coverage is limited in some areas due to existing field development facilities. Unfortunately, those areas are among the most interesting, as they are proven petroleum producing areas. The only 3D survey with good coverage over the platforms is the oldest, acquired in 1997. In order to have good seismic coverage over the predefined imaging area, we used both surveys along with three others that were acquired in 2002, 2004, and 2007. Due to their acquisition setups being largely different, we performed a survey matching using the 2020 survey as reference. Additionally, we conditioned the data for FWI with a 3x9 (gun x channel) array stacking (Bakulin et al., 2018) to enhance the low frequency signals (Figure 1). Due to the geological complexity and the lack of a good starting model, we first used travel-time based FWI (TT-FWI) (Wang et.al., 2018) where time errors become local measurements as a function of time and space. It helps mitigate cycle-skipping issues and thus relaxes the requirements for good starting models and low frequency data. TT-FWI local travel-time mismatches are minimized during the velocity update. As the velocity model is further developed, we introduce Least Square FWI into the workflow to capture details in the velocity model carried by amplitude and waveform variations.

10.1190/image2022-3751051.1

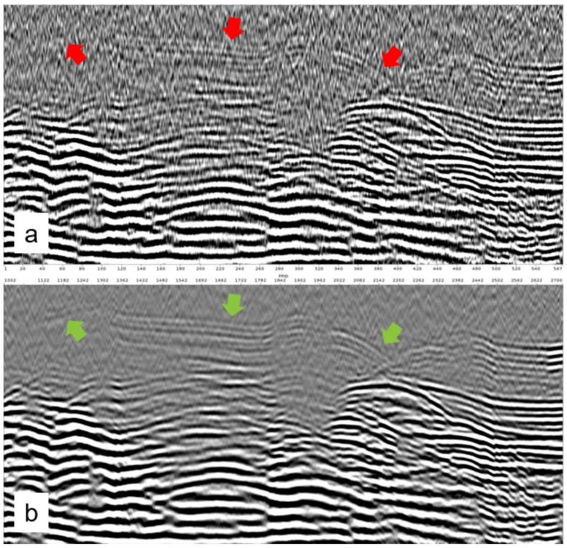

Figure 1: 10-20 Hz low-pass filtered field data at 2,500m offset: raw (top) and conditioned (bottom). Seismic conditioning largely improves the S/N ratio of the target events for FWI.

This area is characterized by fast velocity bodies located in the shallow to mid-depth region of the subsurface. The diapirs of "salt walls" are present at typically less than 500 m depth. The Madiela carbonate formation can also be seen as shallow as 600 m depth in the southern part of the survey. The lack of fast velocity bodies in the starting model may cause a significant cycle-skipping problem that is even challenging to TT-FWI. Inspired by the successful application presented by Cobo et al. (2021), we introduced first-arrival TT-FWI (FA-FWI) to overcome this issue. The cost function is built on the travel-time differences of the first arrival. Fast velocity bodies that generate the fastest traveling recorded arrivals drive the inversion and are thus captured in the model. Powered by a neural network trained first arrival picker, we achieve high fidelity first arrival picking for the entire survey in a very short time.

Although there are 8 km offsets of data and the imaging target is about 1.8 to 2 km in depth to which refraction energy should penetrate in theory, the high velocity contrast (> 3000 m/s) delineating the Madiela formation with thickness of a few hundred meters on average, prevent the deep penetration of diving wave energy. However, the imaging accuracy of the Madiela formation and Ezanga salt formation below is critical to the success of this seismic program. Their fast velocities have a substantial impact on the positioning of the Gamba target immediately underneath. Taking advantage of the strong Madiela and Ezanga salt reflected energy, we apply Born Reflection FWI (Wang et al., 2019) to solve for their velocities with high resolution. Data preprocessing steps for RFWI include denoise, source and receiver 3D de-ghosting, de-signature, survey matching, and 3D surface-related multiple attenuation. We start from a velocity that was developed from several iterations of multi-azimuth tomography and refraction FWI for the overburden, interpretations of top Madiela and top Ezanga, and initial Madiela and Ezanga salt velocities from well-driven acoustic inversion. The well-driven acoustic inversion P-wave velocity model ensures its geological conformity. We apply RFWI from 5 to 10 Hz following a similar workflow as presented by Cobo et al. (2018) and Jones et al. (2019).

Other than the accuracy of the velocity fields, another key element that can affect the resolution of the seismic image is the Earth's absorption quantified by the seismic quality factor, Q. Although there is no evidence from the data nor from experience that there is a local low-Q shallow anomaly such as a gas pocket in the area of interest, we believe the intrinsic Q effect of the overburden sequences limits the resolution of the target. To maximize the resolution of the pre-salt targets, we perform Q-tomography, targeting regional background Q variations. We apply Q-tomography after the velocity model is reasonably established so the kinematic image distortion is minimized. We follow a similar workflow as presented by Sun et al. (2014) where we estimate the Q-factor on Kirchhoff PSDM gathers. We use the sediment velocity scaled Q model as the starting model because the Q-factor is generally proportional to velocity, and we take advantage of the geological conformity in the velocity model. We exclude fast-velocity bodies with complex geometry such as salt and carbonate for two reasons. First and most importantly, kinematic distortions are relatively large around those bodies which results in a bias in the spectral analysis in Q-tomography. Second, they normally have a high Q, which is not of particular interest to seismic imaging.

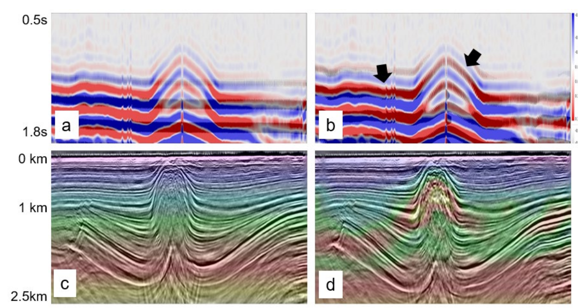

Figure 2: Data matching QC before (a) and after (b) the FA-FWI. Kirchhoff migration QC shows its capability of decent positioning for fast bodies (d) from simple gradient input model (c).

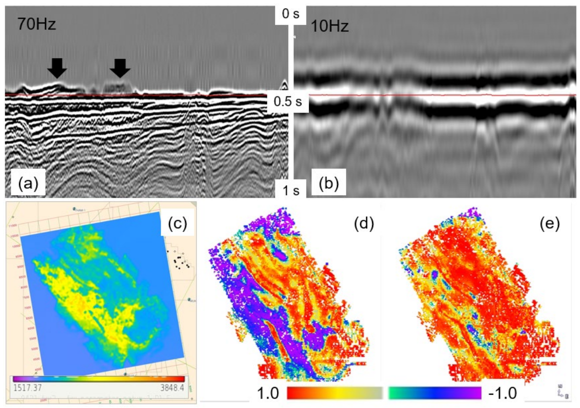

Figure 3: Field data with full bandwidth at 500m offset (a) shows clear refractions which is not distinguishable at 10 Hz (b). High frequency FWI produces high resolution near-surface velocity. Its depth slice at 500m (c) shows that the high velocities match closely with the area where cross-correlation is poor prior to the update (d). The application of the FWI largely improves the cross-correlation (e).

Examples

We apply the FA-FWI in two stages of the velocity model building workflow. First, starting from an initial simple gradient model, we apply it from 5 to 8 Hz to delineate the

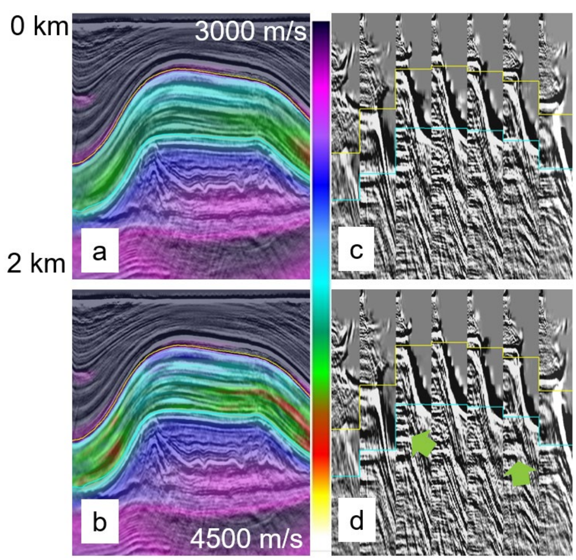

Figure 4: Reflection FWI inside Madiela extracts velocity detail that follows geology and improves gather flatness. (a) and (c) are the Kirchhoff image and gathers, respectively, prior to RFWI. (b) and (d) are their counterpart after RFWI.

general geometry of the fast bodies and the overall positioning. With this update, we also get a coarse update of the sediment velocity. Figure 2a shows the FWI forward modeling QC of a common channel display at 2 km offset with the starting model. The red-blue events in the background are the field data and the overlaying wiggles are the FWI modeled events. With the simple velocity gradient, both sediment and salt refractions are not matched. FA-FWI largely improves the match as shown in Figure 2b. Figure 2c and 2d show the Kirchhoff PSDM image before and after the FA-FWI. We can see, in Figure 2d, that the fast velocities associated with the salt body and Madiela formation are accurately delineated.

While FA-FWI finds major updates for most of the survey and achieves the goal of locating shallow fast bodies, we notice that the matching is systematically poor on the western portion of the survey. Figure 3d shows the cross-correlation QC after FA-FWI at 500 m offset that the western edge of the survey show poor correlation between field data and FWI modeled data, suggesting velocity errors. Further investigation show that there are fast velocity bodies at the near surface at the problematic area that have not been captured. The near surface fast velocity bodies generate refraction energy that is clearly observed at 70 Hz (Figure 3a). However, at 10 Hz which FWI would normally focus on, we do not see the fast velocity refraction as a separate event from the direct arrival (Figure 3b, red line indicates direct arrival time). This tuning effect causes cycle skipping that leads to incorrect velocity updates. We apply FA-FWI at 70 Hz specifically to the near surface and achieve high resolution near surface velocity updates. Figure 3c shows the depth slice at 500 m depth of the updated velocity. We see high velocities up to 3,200 m/s, much faster than what the near-surface sediment velocity would normally be. We observe a strong correlation between the outline of the near-surface fast velocities and that of the previously poor cross-correlation QC (Figure 3c – Figure 3d). With this high frequency FWI, we achieve a greatly improved match with the field data (Figure 3e). Figure 4a and Figure 4b show the RFWI update inside the Madiela formation. RFWI puts detail in the velocity model which is conformable to the inner-Madiela structures. Figure 4c and Figure 4d show the Kirchhoff PSDM gathers before and after the RFWI update, respectively. The RFWI update generates flatter gathers which would be challenging to reflection tomography given the short offset spread and noise contamination.

With a reasonably established velocity model, we apply Q-tomography to solve for the background Q variations. Figure 5a shows the regular Kirchhoff PSDM image and Figure 5b shows the Q-Kirchhoff PSDM image. Figure 5c shows the image with overlying tomo-derived Q model. We detect a low Q area in the shallow section as indicated by the white arrow in Figure 5c. In general, the Q model conforms to the geology. Q-migration largely improves the seismic

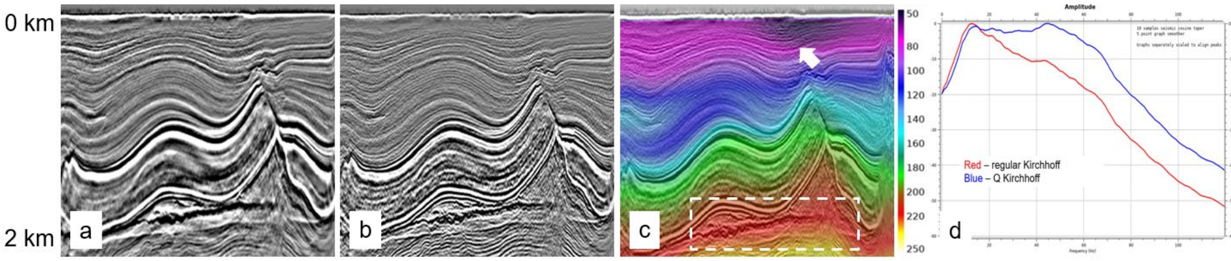

Figure 5: Q-migration (b) largely improves the seismic resolution compared to the regular migration (a). At the target level as measured in the white box in (c), Q-migration achieves a flat spectrum up to 45 Hz, a 10 dB gain (d). The Q model (c) is geologically conformable and detects the near surface, low Q area.

resolution. We measure the amplitude spectrum at the target level as indicated by the white dashed box and observe a flat spectrum up to 45 Hz and up to a 15 dB gain at 60 Hz on the Q-migration image, compared to the regular image (Figure 5d).

Finally, we compare our final image with the legacy product. As presented in Figure 6, we observe great improvements. The current image is seamless, broadband, with high resolution, and obtained form of geologically conformable velocity model. We achieve the objectives set at the beginning of this seismic program.

Conclusions

We presented a velocity model-building case study for multi-azimuth towed streamer data offshore Gabon which makes use of both diving wave and reflection FWI. We achieved a seamless and high-resolution velocity model despite the challenges from complex salt and carbonate geometries. Powered by Q-tomography and Q-migrations, we delivered high granularity imaging of the morphology of the Ezanga salt and fault blocks underneath. The large uplifts mitigate reservoir integrity risks and support petroleum system assessment to reduce prospecting and drilling risks.

Acknowledgement

We would like to thank Vaalco and their partners Addax and Petroenergy for permission to publish the results. We appreciate the ION management for support and permission to present the work. We thank our colleagues and project team members for fruitful discussions and dedication in producing the results presented.

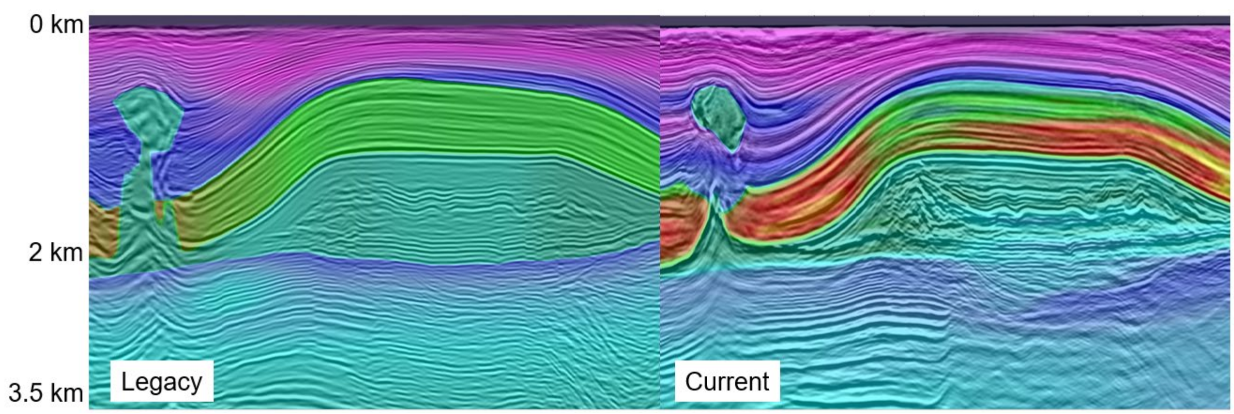

Figure 6: Current image is greatly improved from the legacy. It is seamless and well calibrated. It provides high granularity imaging of the morphology of the Ezanga salt and fault blocks underneath.

REFERENCES

Bakulin, A., P. Golikov, M. Dmitriev, D. Neklyudov, P. Leger, and V. Dolgov, 2018, Application of supergrouping to enhance 3D prestack seismic data from a desert environment: The Leading Edge, **37**, 200–207, doi: https://doi.org/10.1190/tle37030200.1.

Cobo, Y., C. Calderón-Macías, and S. Chi, 2018, Improving model resolution with FWI for imaging and interpretation in a Gulf of Mexico dataset: 88th Annual International Meeting, SEG, Expanded Abstracts, 1108–1112, doi: https://doi.org/10.1190/segam2018-2997675.1.

Cobo, Y., R. F. Fuck, C. Calderon, P. Farmer, and C. Wang, 2021, Assessing sparse-node geometries with full- waveform inversion for a deep water play in Santos Basin: Presented at the First International Meeting for Applied Geoscience & Energy, SEG/AAPG, Expanded Abstracts, 742–746, doi: https://doi.org/10.1190/segam2021-3594936.1.

Gill, J., and D. Cameron, 2002, 3D revives an old play: An Aptian subsalt discovery, Etame field, offshore Gabon, West Africa: The Leading Edge, **21**, 1147–1151, doi: https://doi.org/10.1190/1.1523748.

Jones, I. F., J. Singh, J. Chigbo, P. Cox, C. Hawke, D. Harger, and S. Greenwood, 2019, High resolution velocity and impedance estimation using refraction and reflection FWI: The Fortuna region, offshore Equatorial Guinea: 89th Annual International Meeting, SEG, Expanded Abstracts, 1325–1329, doi: https://doi.org/10.1190/segam2019-3201697.1.

Sun, S. Z., Y. Wang, X. Sun, H. Yue, W. Yang, and C. Li, 2014, Estimation of Q-factor based on prestack CMP gathers and its application to compensate attenuation effects: 84th Annual International Meeting, SEG, Expanded Abstracts, 3709–3714, doi: https://doi.org/10.1190/segam2014-1431.1.

Wang, C., P. Farmer, D. Yingst, I. Jones, G. Martin, and J. Leveille, 2018, Traveltime based reflection full waveform inversion: 80th Annual International Conference and Exhibition, EAGE, Workshop Programme, cp-556-00005.

Wang, C., P. Farmer, T. Burley, C. Calderon, I. Jones, and J. Brittan, 2019, Preconditioned reflection full waveform inversion for subsalt imaging: 89th Annual International Meeting, SEG, Expanded Abstracts, 1214–1218, doi: https://doi.org/10.1190/segam2019-3215997.1.